Research Article

Extension of BET theory to CO_2 adsorption isotherms for ultra-microporosity of covalent organic polymers

Ahmad Mukhtar[1] · Nurhayati Mellon[1] · Sidra Saqib[2] · Siew-Pei Lee[1] · Mohamad Azmi Bustam[1]

Abstract

Usually, nitrogen and argon adsorption–desorption isotherms are used at their respective boiling points for the determination of specific surface area via the BET theory of microporous materials. However, for ultra-micropores, where nitrogen and argon cannot access at cryogenic temperatures, the CO_2 adsorption–desorption isotherms have been considered as alternative options for the determination of specific surface area by extending BET theory, but the surface area determined by using CO_2 adsorption–desorption isotherms is not significant due to strong CO_2-CO_2 interactions. In this study, the microporous covalent organic polymers are subjected to nitrogen and CO_2 adsorption–desorption isotherms and the results showed that a clear linear region is available in isotherms, which confirms the presence of ultra-micropores. The surface area determined by the CO_2 adsorption–desorption isotherms is higher than the surface area determined by N_2 adsorption–desorption isotherms. These results indicate that the microporous covalent organic polymers contain ultra-micropores where only CO_2 can reach, while nitrogen and argon cannot access at cryogenic conditions because their kinetic diameter is larger than CO_2.

Keywords Covalent organic polymers · BET theory · Adsorption–desorption isotherms · Ultra-microporosity · Surface area

1 Introduction

The surface area of porous materials is one of the significant properties because it significantly influences the performance of porous adsorbents in many applications including gas adsorption capacity [1–4], catalysis [5–7], and gas separations [8–11]. Brunauer–Emmett–Teller (BET) [12, 13] technique is one of the most prominent analyses based on argon or nitrogen gas adsorption–desorption isotherms to determine the surface of microporous materials [14], such as zeolites [15], metal–organic frameworks (MOFs) [16], and covalent organic polymers (COPs).

Most of the porous materials have pore texture properties generated from their specific synthesis methods such as (1) precursor particles originated from a solution that produces agglomeration and results a porous structure, (2) synthesis of crystalline compounds such as zeolites or other through hydrothermal crystallization, where the particular arrangement of building blocks yields intra-crystalline pores of molecular size, (3) the thermal treatments including burning or evaporation which may eliminate the volatile compounds or impurities and produce pores as a result of both exist ways of eliminated materials and solid rearrangements, and (4) the selective dissolution of some components that can produce molecular size cavities [17, 18]. Therefore, most of the porous materials are classified into four major groups based on their pore size including micropores (< 2 nm), ultra-micropores (< 0.7 nm), mesopores (2 nm < pore size < 50 nm), and macropores (> 50 nm) [19, 20].

✉ Nurhayati Mellon, norhaye@utp.edu.my | [1]Department of Chemical Engineering, Universiti Teknologi PETRONAS, 32610 Perak, Malaysia. [2]Department of Chemical Engineering, COMSATS University Islamabad (CUI), Lahore Campus, Punjab 54000, Pakistan.

Some of the researchers have questioned the applications of BET theory to the microporous materials because the origin of this theory is based on the gas adsorption–desorption on flat surfaces of adsorbent materials. From a simulation study carried out by Walton et al. [21], they proposed that BET theory can be applied for the determination of the surface area of porous materials containing micropores with a size in the range of $(7-20\times10^{-10}$ m) [22, 23]. Hence, this work aims to investigate the application of BET theory on CO_2 adsorption–desorption isotherms for the surface area determination for covalent organic polymers (COPs) containing ultra-micropores.

2 Materials and methods

Nitrogen-rich porous covalent triazine-based organic polymer has been used in the work for surface area determination through nitrogen as well as CO_2 adsorption–desorption isotherms via BET analysis. The surface area was determined using N_2 adsorption–desorption isotherms at 77 K and CO_2 adsorption–desorption isotherms at 273 K. The sample is outgassed at 393 K for 3 h to remove moisture contents.

3 Results and discussions

The N_2 and CO_2 adsorption–desorption isotherms obtained were further subjected to the BET analysis as shown in Fig. 1. The results show that according to the IUPAC classification of adsorption isotherms [24], the N_2 isotherm resembles the type III having sharp adsorption capacity while indicating the presence of broader pore size distributions, narrower mesopores, and wider micropores. The small hysteresis present in the N_2 adsorption–desorption isotherm is an indication of the capillary condensation phenomenon indicating the mesoporous nature [25]. There is no significant hysteresis observed in the CO_2 adsorption–desorption isotherms which is an indication of easy desorption of the CO_2 molecules because of thermal vibrations of molecules that are in agreement with the reported studies [26, 27].

To investigate the application of BET theory for surface area determination using CO_2 adsorption isotherms, we followed a method reported by Walton and Bae [21, 28]. The BET theory was applied to CO_2 adsorption isotherm by plotting a graph between x as a function of the x axis and $x/q(1-x)$ as a function of the y-axis, where x is P/P_o for CO_2 at 273 K and q is the adsorption capacity of CO_2 over COP. The intercept of the plot yields $[c-1/q]$, while the slope yields $[1/qc]$ in the linear region of the plot. To satisfy these criteria of calculating surface area, two conditions must be fulfilled: (1) the value of $q(P-P_o)$ should be increased with increasing x, and (2) the y intercept in the linear region of the graph must yield a positive value, which must be greater than zero to get the meaningful value of c. Finally, the surface can be calculated using Eq. 1:

$$A = q \times \sigma_o \times N_{AV} \qquad (1)$$

where q is the adsorption capacity of CO_2 at 273 K, σ_o is the cross-sectional area of CO_2 at 273 K, which is 21.8×10^{-10} m, and N_{AV} is the Avogadro's number, which is 6.022×10^{23} mol^{-1}.

The graphical representation of this method is presented in Fig. 2. The surface area from CO_2 adsorption isotherm is calculated using Eq. (1) at 273 K and from N_2 adsorption isotherm at 77 K which is tabulated in Table 1. We now investigate the surface area determination using CO_2 adsorption isotherms only in the linear region because the linearity of the BET plot is a key factor for the determination of the accurate specific surface
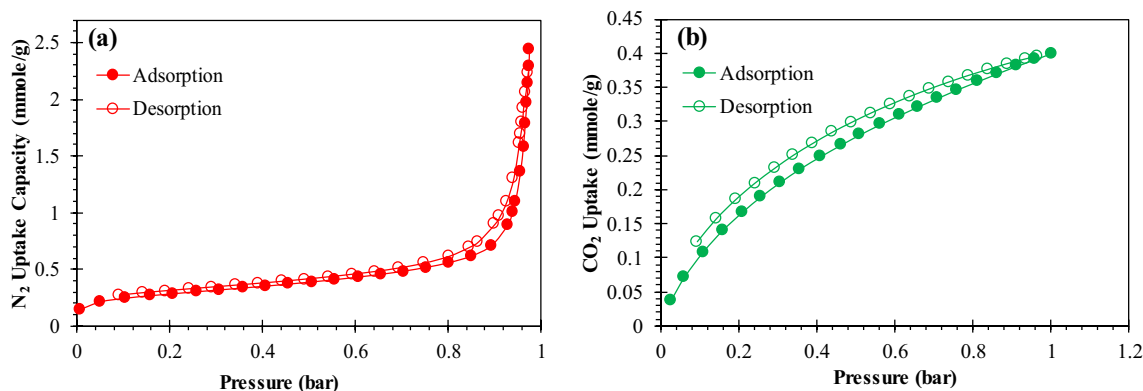

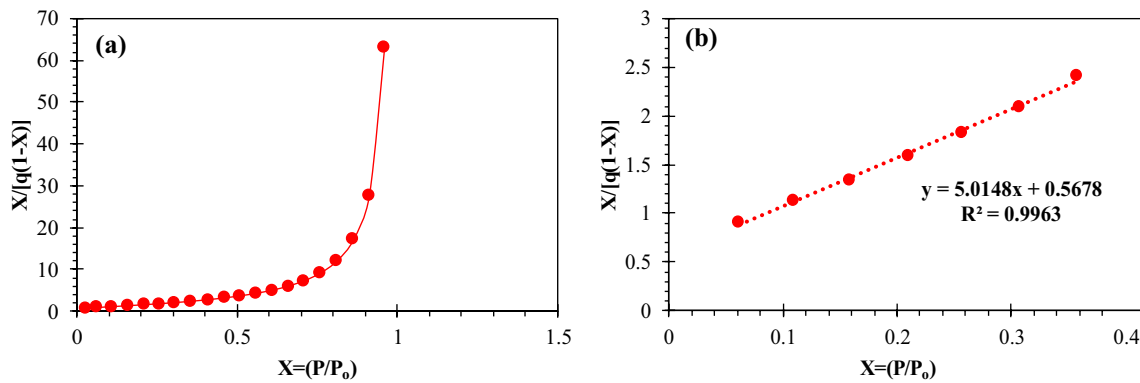**Fig. 1** N_2 and CO_2 adsorption–desorption isotherms at 77 K and 273 K, respectively

Fig. 2 Application of BET theory on CO_2 adsorption isotherms at 273 K

Table 1 BET surface area calculated by applying BET theory on N_2 and CO_2 adsorption isotherms

Material	S_{BET} (m^2/g) from N_2 isotherm	S_{BET} (m^2/g) from CO_2 isotherm	References
COP	22	23	This work
MOF-177	1721	47	[29]
MOF-200	3624	1265	[30]
MOF-200/GO	3359	167	[30]

area of porous materials. Since the selection of a linear region in the convex or concave-shaped plot is not difficult, it can be identified easily. However, in the selection of the linear region, it must be considered that the linear range should be in the low pressure range and there should not be any overshooting in CO_2 adsorption capacity. The results clearly show that the surface area calculated from CO_2 adsorption isotherms at 273 K is higher than the surface area calculated using N_2 adsorption isotherm at 77 K. It can be considered that surface area calculated by CO_2 adsorption isotherm may be accounted for the ultra-microporosity because of its small kinetic diameter than N_2 molecules. However, the diffusional resistances due to the temperature of the adsorption process are one of the significant parameters which affect the reach of adsorbate molecules into the ultra-micropores. The results are in agreement with the previously reported studies [21]. In comparison with the reported literature, Sami et al. [29] and his coworkers reported the experimental investigation of the ultra-microporosity determination in a metal–organic framework (MOF-177) by employing the CO_2 adsorption for BET technique. The results revealed that the absence of any ultra-micropores in the MOF-177 as the specific surface area of the MOF-177 was reduced from 1721.09 to 47.4739 m^2/g when N_2 and CO_2 gases were used for BET technique, respectively. Similarly, in another work, Sami et al. [30] and his coworkers reported

the ultra-microporosity analysis of the two metal–organic frameworks: one was unfunctionalized (MOF-200) and one was functionalized with the graphene oxide (MOF-200/GO). The results again demonstrated the loss of the specific surface areas of both metal and organic frameworks, i.e., MOF-200 (1265 m^2/g) and MOF-200/GO (167 m^2/g) from MOF-200 (3624 m^2/g) and MOF-200/GO (3359 m^2/g). This was an indication of the absence of any ultra-micropores in the MOF-177 as the surface area of the MOF-177 was reduced from 1721.09 to 47.4739 m^2/g when N_2 and CO_2 gases were used for BET technique, respectively. However, both reported studies revealed that the reported method can be employed for the ultra-microporosity analysis.

4 Conclusion

In this study, a porous covalent organic polymer (COP) was subjected to the BET analysis to investigate the application of BET theory for specific surface area determination using N_2 adsorption isotherm at 77 K and CO_2 adsorption isotherm at 273 K. The results showed that the surface area determined by using the CO_2 adsorption isotherms was higher than the surface area determined by using the N_2 adsorption isotherms. The results provided a clear indication of the presence of an ultra-microporous region in the microporous structure. The results recommend the meaningfulness of CO_2 adsorption isotherms for the surface area determination in the ultra-microporosity using BET theory. Future research can be carried out to investigate the comparative effect of the kinetic diameter of the adsorbate molecule and diffusive resistance due to the temperature of the adsorption process on the ultra-microporosity.

Compliance with ethical standards

Conflict of interest The authors have not any conflict of interest regarding the publication of this paper.

References

1. Yuan D (2015) Porous materials to store clear energy gases. Adv Nanomater Appl Renew Energy. https://doi.org/10.1016/B978-0-12-801528-5.00006-3
2. Han SS, Goddard WA (2007) Lithium-doped metal-organic frameworks for reversible H2 storage at ambient temperature. J Am Chem Soc 129:8422–8423
3. Ma S, Zhou H-C (2010) Gas storage in porous metal–organic frameworks for clean energy applications. Chem Commun 46:44–53
4. Collins DJ, Zhou H-C (2007) Hydrogen storage in metal–organic frameworks. J Mater Chem 17:3154–3160
5. Vermoortele F, Vandichel M, Van de Voorde B, Ameloot R, Waroquier M, Van Speybroeck V et al (2012) Electronic effects of linker substitution on Lewis acid catalysis with metal–organic frameworks. Angew Chem Int Ed 51:4887–4890
6. Ma L, Abney C, Lin W (2009) Enantioselective catalysis with homochiral metal–organic frameworks. Chem Soc Rev 38:1248–1256
7. Nguyen HGT, Weston MH, Farha OK, Hupp JT, Nguyen ST (2012) A catalytically active vanadyl (catecholate)-decorated metal organic framework via post-synthesis modifications. CrystEngComm 14:4115–4118
8. Wang B, Côté AP, Furukawa H, O'Keeffe M, Yaghi OM (2008) Colossal cages in zeolitic imidazolate frameworks as selective carbon dioxide reservoirs. Nature 453:207
9. Thallapally PK, Tian J, Radha Kishan M, Fernandez CA, Dalgarno SJ, McGrail PB et al (2008) Flexible (breathing) interpenetrated metal–organic frameworks for CO₂ separation applications. J Am Chem Soc 130:16842–16843
10. Couck S, Denayer JF, Baron GV, Rémy T, Gascon J, Kapteijn F (2009) An amine-functionalized MIL-53 metal–organic framework with large separation power for CO₂ and CH₄. J Am Chem Soc 131:6326–6327
11. Bae YS, Snurr RQ (2011) Development and evaluation of porous materials for carbon dioxide separation and capture. Angew Chem Int Ed 50:11586–11596
12. Lowell S, Shields JE, Thomas MA, Thommes M (2012) Characterization of porous solids and powders: surface area, pore size and density, vol 16. Springer, Berlin
13. Brunauer S, Emmett PH, Teller E (1938) Adsorption of gases in multimolecular layers. J Am Chem Soc 60:309–319
14. Chui SS-Y, Lo SM-F, Charmant JP, Orpen AG, Williams ID (1999) A chemically functionalizable nanoporous material [Cu₃(TMA)₂(H₂O)₃]ₙ. Science 283:1148–1150
15. Wang H, Wang Z, Huang L, Mitra A, Holmberg B, Yan Y (2001) High-surface-area zeolitic silica with mesoporosity. J Mater Chem 11:2307–2310
16. Férey G (2008) Hybrid porous solids: past, present, future. Chem Soc Rev 37:191–214
17. Kaneko K (1994) Determination of pore size and pore size distribution: 1. Adsorbents and catalysts. J Membr Sci 96:59–89
18. Gregg S, Sing AKSW (1982) Surface area and porosity. Academic Press, London
19. Smith DM, Hua D-W, Earl WL (1994) Characterization of porous solids. MRS Bull 19:44–48
20. Unger K, Rodríguez-Reinoso F, Rouquerol J, Sing KS (1991) Characterization of porous solids II, vol 62. Elsevier, Amsterdam
21. Walton KS, Snurr RQ (2007) Applicability of the BET method for determining surface areas of microporous metal–organic frameworks. J Am Chem Soc 129:8552–8556
22. Gelb LD, Gubbins K (1998) Characterization of porous glasses: Simulation models, adsorption isotherms, and the Brunauer–Emmett–Teller analysis method. Langmuir 14:2097–2111
23. Galarneau A, Cambon H, Di Renzo F, Fajula F (2001) True microporosity and surface area of mesoporous SBA-15 silicas as a function of synthesis temperature. Langmuir 17:8328–8335
24. Thommes M, Kaneko K, Neimark AV, Olivier JP, Rodriguez-Reinoso F, Rouquerol J et al (2015) Physisorption of gases, with special reference to the evaluation of surface area and pore size distribution (IUPAC Technical Report). Pure Appl Chem 87:1051–1069
25. Klumpen C, Breunig M, Homburg T, Stock N, Senker J (2016) Microporous organic polyimides for CO₂ and H₂O capture and separation from CH₄ and N₂ mixtures: interplay between porosity and chemical function. Chem Mater 28:5461–5470
26. Espinal L, Wong-Ng W, Kaduk JA, Allen AJ, Snyder CR, Chiu C et al (2012) Time-dependent CO₂ sorption hysteresis in a one-dimensional microporous octahedral molecular sieve. J Am Chem Soc 134:7944–7951
27. Lee S-P, Mellon N, Shariff AM, Leveque J-M (2018) Geometry variation in porous covalent triazine polymer (CTP) for CO₂ adsorption. New J Chem 42:15488–15496
28. Bae YS, Yazaydın AO, Snurr RQ (2010) Evaluation of the BET method for determining surface areas of MOFs and zeolites that contain ultra-micropores. Langmuir 26:5475–5483
29. Ullah S, Bustam MA, Assiri MA, Al-Sehemi AG, Sagir M, Kareem FAA et al (2019) Synthesis, and characterization of metal-organic frameworks-177 for static and dynamic adsorption behavior of CO₂ and CH₄. Microporous Mesoporous Mater 288:109569
30. Ullah S, Bustam MA, Al-Sehemi AG, Assiri MA, Kareem FAA, Mukhtar A et al (2020) Influence of post-synthetic graphene oxide (GO) functionalization on the selective CO₂/CH₄ adsorption behavior of MOF-200 at different temperatures; an experimental and adsorption isotherms study. Microporous Mesoporous Mater 296:110002

Publisher's Note Springer Nature remains neutral with regard to jurisdictional claims in published maps and institutional affiliations.